Computational simulations of stress shielding and bone resorption around existing and computer-designed orthopaedic screws

A. Gefen

Department of Biomedical Engineering, Tel Aviv University, Tel Aviv, Israel

Abstract—*Failure of an orthopaedic fixation due to stress shielding and consequent screw loosening is a major concern among surgeons: the loosened screws could not only interfere with the healing process but also endanger adjacent anatomical structures. In this study, the effect of the screw's engineering design (dimensions, profile shape and material properties) on the load sharing with adjacent bone and consequent bone resorption was tested, using a set of two-dimensional computational (finite element) models. An algorithm simulating local bone adaptation to strain energy density (SED) mechanical stimuli was developed and used to evaluate the biomechanical performances of different commercial screws. Two new designs, a 'graded-stiffness' composite screw, with a reduced-stiffness titanium core and outer polymeric threads, and an active-compression hollow screw that generates compressive stresses on the surrounding bone, were also evaluated. A dimensionless set of stress transfer parameters (STPs) were utilised for ranking the performances of the different screws according to the expected screw–bone load sharing and its evolution with adaptation of the surrounding tissue. The results indicated that commercial wide (6 mm thread diameter) trapezoidal and rectangular screw profiles have superior biomechanical compatibility with bone (i.e. predicted to be stable after 2 years). The graded-stiffness and active-compression screws provided the best biomechanical performances: bone loading around them was predicted to decrease by no more than 15% after 3 years, compared with a decrease of 55–70% in bone loading around commercially available screws. Computer simulations of bone adaptation around orthopaedic screws are demonstrated to be effective means for objective and quantitative evaluation of the biomechanical aspects of implant–tissue compatibility.*

Keywords—*Fracture fixation, Bone adaptation, Osseo-integration, Osteosynthesis, Screw design, Finite element method*

Med. Biol. Eng. Comput., 2002, **40**, 311–322

1 Introduction

BONE SCREWS can be used alone or in conjunction with plates to connect fragments of a fractured bone. Surgical use of screws in the stand-alone configuration is accepted for treating reducible intracapsular hip fractures, slipped capital femoral epiphysis, distal femoral condyle and tibial plateau fractures, as well as for treating ankle, elbow and shoulder fractures (PERREN *et al.*, 1992). The screws used in these procedures to achieve interfragmental compression or to stabilise bone transplants are generally termed lag screws.

Progressive loosening of screws used for bone fixation is well-documented in the clinical literature (SKINNER and POWLES, 1986; EVANS *et al.*, 1990; HYLDAHL *et al.*, 1991; PANAGIOTOPOULOS *et al.*, 1994; LOWERY and MCDONOUGH, 1998; WIMMER and GLUCH, 1998). Stress shielding, a mechanical effect occurring in structures combining stiff with more flexible materials, is considered to be the major reason for triggering the loosening process.

Bones in normal, healthy condition carry external joint and muscular loads by themselves. Following the insertion of orthopaedic screws, e.g. for stabilising or for repairing a fracture, the treated bone will share its load-carrying capacity with the screws. Thus the same load that had been originally born by the bone itself will now be carried by the 'composite' new structure.

As the clinically available screws are metallic and therefore significantly stiffer (elastic modulus of around 100 GPa for titanium and up to 200 GPa for steel) than the adjacent bone (modulus of 1–20 GPa), internal loads will be mainly supported by the screws that are now 'shielding' the bone from carrying the normal mechanical stresses. This stress shielding effect alters the normal stress stimuli for bone growth: in accordance with Wolff's law, the reduction of bone stresses relative to the natural situation causes bone to adapt itself by reducing its mass in a process of resorption around the implant. This will

Correspondence should be addressed to Dr Amit Gefen; email: gefen@eng.tau.ac.il

Paper received 6 September 2001 and in final form 7 March 2002

MBEC online number: 20023668

cause micromotion of the screws in response to external loads and could further damage the interfacing bone layer and anchorage performances subsequent to possible loosening of the screw (Fig. 1).

The success of fracture repair or bone transplant stabilisation procedures is mainly dependent upon the holding power of the screws. Early loosening of the screws can not only delay or damage the healing process, but can also endanger adjacent anatomical structures and can even require surgery for the immediate removal of the failed implants (LOWERY and MCDONOUGH, 1998). This would inevitably impose a prolonged and painful rehabilitation process on patients, as well as substantial treatment costs. New screw designs aimed at minimising the undesired stress shielding effect would contribute vastly to solving these problems (GEFEN, 2001; 2002).

Although several other factors (e.g. the biocompatibility of the screw's material, hormonal influences and vascular interruptions) play a role in the resorption of bone around the screw, the experimental data reported in the literature indicate that the role of stress shielding is critical (PILLIAR *et al.*, 1979; TOMITA *et al.*, 1991; HUISKES *et al.*, 1992). Animal (canine) experiments with screw and plate fixation systems have shown that cortical and trabecular bone losses are reduced if a reduced-stiffness implant with identical geometrical design is used (PILLIAR *et al.*, 1979; TOMITA and KUTSUNA, 1987). Moreover, cushioning of the plates with a silicone layer to reduce their overall stiffness and increase stress transfer to bone eliminated underlying bone resorption without decreasing the strength of the fracture fixation (TOMITA *et al.*, 1991).

HUISKES *et al.* (1992) demonstrated that metallic (titanium) hip stems implanted in dogs caused a 20–23% reduction in proximal femoral bone cross-section 2 years post-implantation.

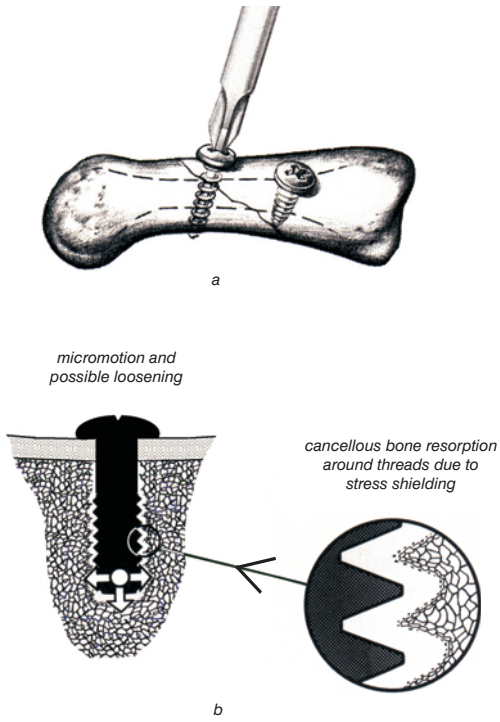

Fig. 1 *(a) Orthopaedic screws are well-known and clinically accepted devices for fracture fixation and bone transplant stabilisation. Crucial problem in creating necessary permanent tissue anchorage of screw for successful fixation is (b) resorption of cancellous bone around screw's threads. Lack of adequate anchorage can result in micromotion and possible gradual loosening of screw, which could lead to failure of fixation*

Recently, ANG *et al.* (1997) compared bone remodelling around metallic and polymeric hip stems in humans using dual energy X-ray absorptiometry (DEXA) and showed greater bone mineral density around the polymeric (less stiff) stems. These experimental findings clearly indicate the role of adequate implant-to-bone stress transfer in maintaining a normal level of adjacent bone mass.

Assuming that the effects of stress shielding on bone remodelling around the screw are, indeed, the dominant ones, and putting other potentially affecting factors aside for the moment, the process of screw loosening can be simulated in isolation by means of biomechanical modelling using stress-adaptive bone remodelling theory (COWIN and HEGEDUS, 1976; HUISKES *et al.*, 1987; 1992; LEVENSTON *et al.*, 1993). This theory is a mathematical formulation of Wolff's law for calculating the net effect of a given stress state on local bone gain or loss. When used in conjunction with finite element (FE) analyses of the stress fields resulting from the screw–bone interaction, this approach can be applied to study the effect of the physical design of bone screws (including dimensions, geometrical shape and material characteristics) on long-term screw stability, as determined by the bone adaptation process.

The reliability of simulations of bone adaptation in the vicinity of orthopaedic implants, e.g. around stems of hip prostheses, was evident in animal experiments in which the observed trabecular bone density and cortical bone morphology changes could be numerically predicted with reasonable detail (HUISKES *et al.*, 1991).

In this study, two-dimensional (2D) computational models of the screw–bone interaction were utilised to simulate stress-related bone adaptation, to characterise screw design parameters and test new screw structures that would provide optimum stress transfer to the surrounding bone, to maintain its mass and thereby maintain the screw's stability.

A reasonable conclusion that can be reached based on the above-listed studies of stress shielding is that orthopaedic fixations should be manufactured with elastic properties that are identical to those of natural bone. Unfortunately, even using state-of-the-art material engineering, it is not yet possible to produce such ideal biocompatible materials with elasticity of around 1 GPa (as for trabecular bone (GUE, 2001)) and with the ultimate material strength required to carry physiological loadings similar to the ones carried by normal bones (σ_{UTS} is around 10 MPa for trabecular bone).

The development of new composite materials or tissue-engineered structures may provide future solutions, but, to date, titanium (with its given stiffness and its beneficial biocompatibility) is the most successful option available for orthopaedic screw manufacturing. Considering the above, an important goal of the present study was to test whether the undesirable effects of stress shielding of titanium implants can be reduced, by optimising additional design parameters of the screw. The screw's thread profile is of particular importance in optimising the load transfer (EVANS *et al.*, 1990), but there are no literature reports of a quantitative, objective and comparative evaluation of the load transfer performances of basic thread profiles (triangular, rectangular and trapezoidal).

As this is the first study to make such a comparative quantitative evaluation, it was necessary to test many combinations of thread shapes in titanium screws and to alter their number, to analyse the effect on the load sharing, which was quantified by a newly developed parametric approach. This approach, which provides a dimensionless representation of the screw-to-bone stress transfer over time, with the consequent adaptation of bone, was used to predict the long-term quality of the fixation and screw's stability, as determined by the intensity and pattern of bone resorption around specific existing and novel screw designs.

2 Methods

2.1 *General comments*

For the purpose of predicting the long-term response of bone tissue to the insertion of a screw, a computational formulation of adaptive bone remodelling theory was used in combination with FE modelling. The computer simulation procedure can be outlined as follows. The FE analysis provided the stress and strain distributions in idealised and proximal femur bone structures (Fig. 2). From the stress and strain distributions, a mechanical stimulus ((2) below) was determined for each bone tissue element. The stimulus controlled the remodelling rate of the bone element for which it was calculated, according to a relationship specified by a remodelling rule (3). The bone element's density was then related to its elasticity, to create an updated input of bone density distribution for the FE model (1). The iterative process stopped when a steady state was reached, i.e. when the difference between the density fields predicted in two consequent iterations dropped below a pre-defined threshold (HUISKES *et al.*, 1987; 1992).

The results produced by the two FE model types (Fig. 2) were used to provide details for application in the design considerations that are expected to improve the screw's biomechanical performances, with the aim of achieving more stable, long-lasting fixations. Particular emphasis was placed on the development and computational evaluation of new bone screw designs that are potentially capable of loading the surrounding bone more efficaciously than commercially available screws, by providing optimum mechanical stimuli for bone growth and healing.

2.2 *Algorithm for bone adaptation simulations*

Although conventional FE models of the musculoskeletal system provide detailed information on internal stress distributions, they reveal nothing about the long-term effects of changes

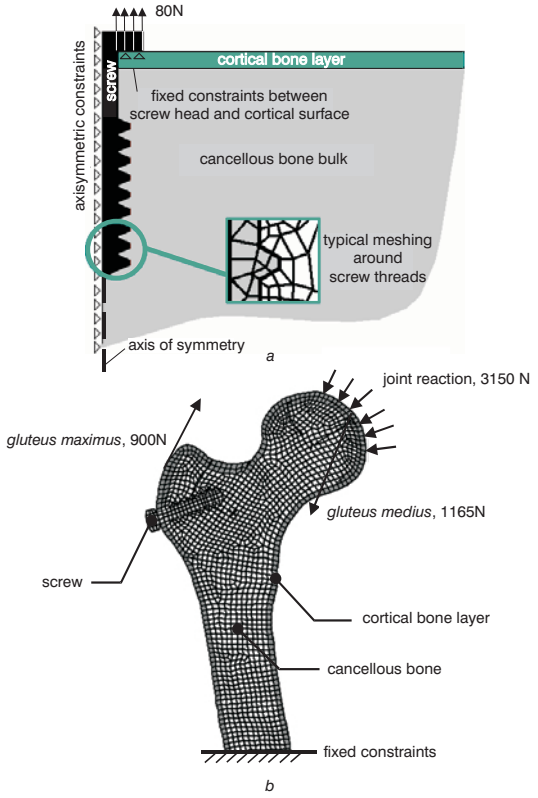

Fig. 2 *2D computational modelling of bone–screw mechanical interaction: (a) representative idealised model and (b) femoral head model*

in bone stresses. The coupling of the FE method with a quantitative bone remodelling theory allows the study of both the stress state and the internal bone morphology, as changes occur simultaneously in both (HUISKES *et al.*, 1992; LEVENSTON *et al.*, 1993; TERRIER *et al.*, 1997). Fig. 3*a* depicts the algorithm by which Wolff's law was customised to simulate cancellous bone adaptation in the presence of a screw. Starting from a 2D homogenous distribution of bone stiffness and density, i.e. apparent densities of 1.85 and 0.9 g cm^{-3} for the cortical and cancellous components, respectively, an incremental time-dependent technique was employed to simulate the evolution of cancellous bone density distribution around the implant. The elastic moduli per element E (MPa) were determined from the density values ρ, according to the relationship

$$E = \alpha\rho^3 \tag{1}$$

where α is a constant taken as 2875 MPa cm^3 g^{-1} (CARTER and HAYES, 1977).

The FE software package (NASTRAN) was integrated with a stress adaptive bone remodelling simulation procedure (Fig. 3a). The simulation was based on a conservative formulation of the adaptive remodelling theory that assumes that the bone reacts only to differences above a predetermined threshold value between the actual stress/strain in the bone following insertion of the screw and the stress/strain in the intact, healthy bone (COWIN and HEGEDUS, 1976; HUISKES *et al.*, 1987; 1992). This process requires the definition of a remodelling signal that represents the stress stimulus for net bone remodelling and the setting of a remodelling rule that is the mathematical description of the density gain/loss process.

The local stress stimulus ψ applied to a 2D bone tissue element near the screw can be expressed as (CARTER *et al.*, 1989; VAN REITBERGEN *et al.*, 1993)

$$\psi = \frac{U}{\rho} = \frac{\int_A(\sigma_x\varepsilon_x + \sigma_y\varepsilon_y + \tau_{xy}\gamma_{xy})dA}{2\rho} \tag{2}$$

where U is the strain energy density (SED). The SED was calculated for a 2D stress state using the values of the normal stresses σ_x, σ_y, the shear stress τ_{xy}, the normal strains ε_x, ε_y and the shear strain γ_{xy}. For each bone element and during each step of the simulation, the threshold level for the remodelling response (Fig. 3*b*), ω was compared with the absolute difference $|\psi - \psi_{ref}|$ between the stress stimulus following the screw's implantation ψ and the stimulus normally applied to the intact bone ψ_{ref}. If the difference $|\psi - \psi_{ref}|$ was smaller than ω, it was assumed that no remodelling response would occur. Accordingly, a remodelling rule (depicted in Fig. 3*b*) can be formulated by (TERRIER *et al.*, 1997),

$$\frac{d\rho}{dt} = \begin{cases} c(\psi - \psi_{ref}) + c\omega & (\psi - \psi_{ref} < -\omega) \\ 0 & -\omega \leqslant \psi - \psi_{ref} \geqslant +\omega \\ c(\psi - \psi_{ref}) - c\omega & (\psi - \psi_{ref} > +\omega) \end{cases} \tag{3}$$

where c is an empirical rate constant, and ω is the half-width of the central, normal activity region (below the threshold for remoulding response), which is commonly termed the 'dead zone'. For the numerical simulations, we followed BEAUPRÉ *et al.* (1990) and assumed that a local effective stress of 150 MPa day^{-1} would result in a linear apposition rate of 3.0 μm day^{-1}. Based on this assumption, $c = 0.02$ (μm day^{-1})/(MPa day^{-1}). The value of the dead zone width 2ω was also determined, according to BEAUPRÉ *et al.* (1990), to be 30 MPa.

After the stress field in the initial, homogenous model was solved, the apparent density of each bone element was updated according to (3), and the resultant changes in the local elastic moduli were calculated from (1). If a local density of the cancellous bone reached the maximum value $\rho_{max} = 1$ g cm^{-3},

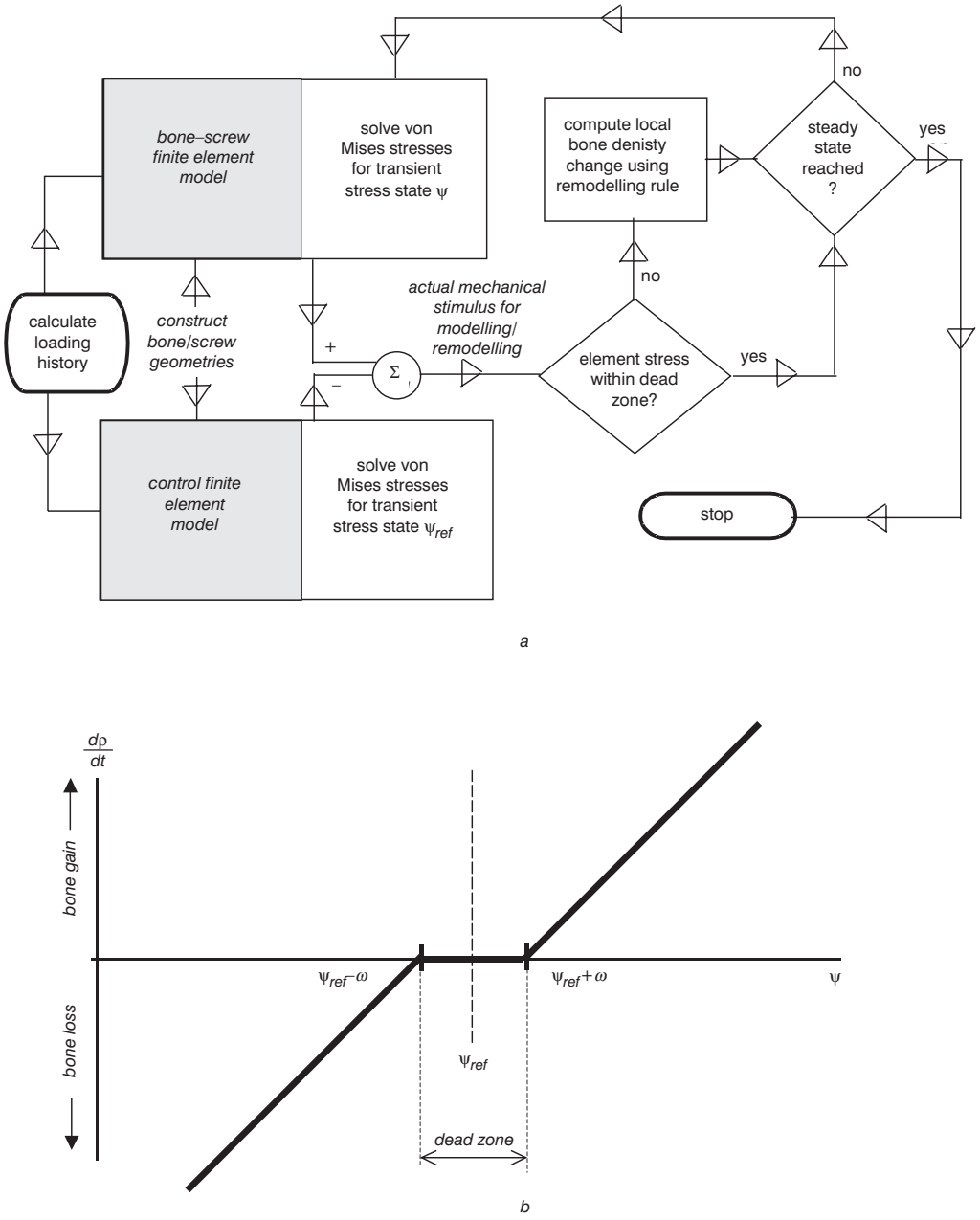

Fig. 3 *Outline of bone adaptation simulation procedure: (a) flowchart of iterative remodelling algorithm; (b) schematic diagram of remodelling rule (3) applied to piecewise linear remodelling rate relationship that contains 'dead zone' non-linearity*

it was assumed that no further local gain of bone mass could occur. Similarly, the minimum value for the local cancellous bone density was set to $\rho_{min} = 0.01\,g\,cm^{-3}$, which represented complete local resorption. The Poisson ratio for each bone element was kept constant at 0.35, throughout the complete simulation process (MOW and HAYS, 1997).

So that convergence could be reached, the process described in Fig. 3*a* was continued until no further significant density/stiffness changes occurred. This meant that, either the densities in all the bone elements had evolved according to (3), or that they had reached the maximum or minimum values of tolerable cancellous density (1 and $0.01\,g\,cm^{-3}$, respectively), and, in addition, the difference between the density field of the final iteration n and the previous iteration $n-1$ did not exceed 1%.

2.3 *Bone screw specifications*

The remodelling algorithm described above and related FE simulations were employed for analysis of the predicted bone response to the insertion of fixation screws continually over time. The geometric and material characteristics of the screws were modelled to represent typical designs that are currently available commercially, in an attempt to rate the likelihood of loosening of screws with these designs and to identify preferred specifications.

Several basic dimensions were set at a constant throughout the simulations: a shaft diameter of 2 mm, a screw-head diameter of 6 mm and a thread pitch of 1 mm. Other design parameters were altered so that the consequent changes in the simulated adaptation behaviour of bone could be analysed and so that these effects on the predicted long-term stability of the studied screw could be explored. Accordingly, the length of the screw's shaft (i.e. without the head and threads) was set at 25 mm (short) or at 75 mm (long), the profile of the threads was modelled as having a triangular, rectangular or trapezoidal shape, the thread diameter was set at 4 mm (regular) or 6 mm (wide), and the number of threads was 4, 5, 8 or 9 (hence, the range of tested screw lengths was 33–88 mm). The screws were assumed to be made of

standard titanium alloy (Ti-6A1-4V), with an elastic modulus of 105 GPa and a Poisson ratio of 0.35, or, alternatively, to be made of reduced-stiffness titanium, with a modulus of 40 GPa.

The biomechanical performances of two newly proposed designs, presented in Fig. 4, were also evaluated. The first was a graded-stiffness composite screw (Fig. 4*a*) integrating two different material components: one was a low-stiffness-titanium core with an elastic modulus of 40 Gpa, and the other was a polymeric external layer/threads with an elastic modulus of 10 GPa. Orthopaedic fixation is termed *dynamic* when body weight or muscle forces are used to produce compression that is additional to the one produced by the fixation device alone. Commercial dynamic fixation designs (e.g. the Richards sliding hip screw and plate system) provide good clinical results and are now considered a standard treatment of femoral fractures (ADAMS *et al.*, 2001). The more elastic graded-stiffness screw, which mimics more closely the elastic behaviour of bone, can be classified as being a dynamic screw because

(i) it allows development of more physiological strain patterns in the bone surrounding the screw during weight-bearing and functional locomotor activity of the patient
(ii) under these conditions, it is likely to cause smaller obstructions to the already tenuous periosteal and intra-trabecular blood supply in the vicinity of the insertion region, by minimising local stress concentrations at the tissue and transferring functional loads more homogenously. This should improve the conditions for healing of the fractured bone.

The second design was an active-compression hollow screw (Fig. 4*b*) containing a rigid metal sphere. Following the insertion of the screw, the sphere is pushed downward within its canal, thereby causing a slight opening of the screw's tip, an action that leads to transfer of compression stress to the adjacent bone. For modelling purposes, an evenly distributed traction of 5 N was introduced at the distal third of the active-compression screw perpendicularly to its surface, to represent the action of this sphere. The 5 N force value was calculated by modelling the canal wall of the active-compression screw as a cantilever beam subjected to bending owing to the thrusting of the internal sphere (Fig. 4*b*): the maximum bending compression generated within the canal wall of the active-compression screw was limited to 50% of the compressive strength of trabecular bone (~10 MPa), to eliminate potential local tissue damage when this screw was activated.

The profile shape, shaft and thread diameters and other basic design characteristics of the newly proposed graded-stiffness and active-compression screws were reproduced from the commercial screw types that demonstrated the best screw–bone load sharing performances (in the short and long term), as further detailed in Section 3. The adaptation simulations were applied to assess whether a more homogenous screw–bone stress transfer (by means of the graded-stiffness screw) or application of active stress stimuli (by means of the active-compression screw) could influence the remodelling response of the surrounding bone towards achieving greater screw stability for longer periods.

2.4 *Finite element models*

Two types of 2D FE model of screw–bone interaction were utilised for calculating time-dependent bone stresses. The first model type was an idealised axisymmetrical cross-section through a bone cylinder (with an outer cortical surface and an inner trabecular bulk), into which a central bone screw was inserted perpendicularly (Fig. 2*a*). The screw tightening and the screw–bone contact conditions were simulated by the action of axial forces at the screw's interface with the cortical surface. This not only permitted easy creation of models, but also

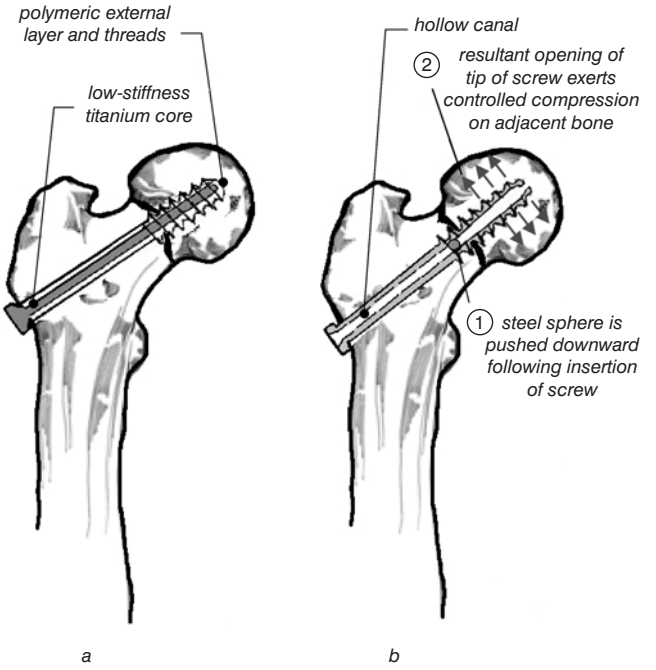

Fig. 4 *Two newly proposed bone screw designs: (a) graded-stiffness screw providing gradual transfer of contact stresses to bone by employing stiffer metallic core surrounded by softer polymeric external layer and threads; (b) active-compression screw providing mechanical stress stimuli for bone mass gain around its tip*

provided a tool for basic comparisons of screw performances by isolating the effects of the screw's engineering design parameters (SCHULLER-GÖTZBURG *et al.*, 1999).

The second model type was a proximal femur that had been implanted with selected screw types (e.g. Fig. 2*b*) to allow evaluations to be carried out in a more complex geometrical structure and loading environment, conditions that are closer to realistic ones. To explore the long-term tissue response, close apposition of bone to the screw (osseo-integration) was assumed to exist initially in both model types. Possible initial bone damage due to surgery, appreciable relative motion or abrasion at the screw–bone interface, which could lead to failure of the implantation in the short-term (ALBREKTSSON, 1985), were not considered in the present study.

Idealised screw–bone models (Fig. 2*a*) were initially developed to isolate the effects of the screw's engineering design on the stress transfer to bone. Performances of the different screws were then tested in a more realistic geometry of the proximal femur (Fig. 2*b*). The following basic components were included in each idealised simulation (Fig 2*a*): compact bone layer, 3 mm in thickness, that is typical of the femur and tibia (SCHULLER-GÖTZBURG *et al.*, 1999), underlying cancellous bone bulk (100 mm width × 250 mm height) and a single fixation screw.

In each simulation, the surface under the screw head was fixed and loaded with a force of 80 N to simulate tightening (SCHULLER-GÖTZBURG *et al.*, 1999). The succeeding model type of a fixative screw inserted into the femoral head (Fig. 2*b*) was aimed to include additional structural factors that could affect the screw-to-bone stress transfer and the consequent remodelling process, e.g. a non-uniform thickness of the cortical layer and more complex skeletal/muscular loading.

The simulated fracture cases included fracture of the femoral neck (for longer screws) and fracture of the greater trochanter (for shorter screws). Fracture lines were not included in the models, as the course of fracture can vary considerably between patients (OMURA *et al.*, 2000), and the present femoral model was intended to serve as a standard benchmark for screw evaluation.

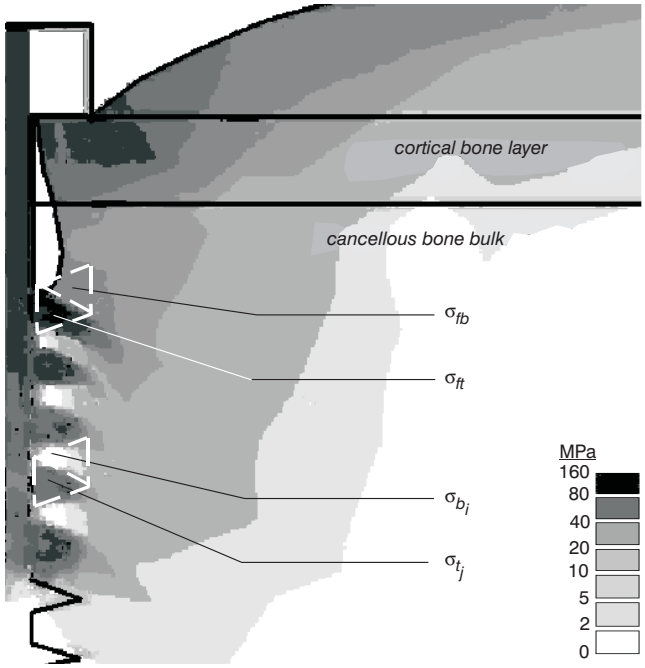

Fig. 5 *Definition of regions for calculating average von Mises screw-thread stress values and average von Mises stress values within cancellous bone volumes that are found between threads, as required for computation of stress transfer parameters (STPs). Example is given for triangular thread profile shape. Bone deformation is magnified (×30) to depict screw–bone mechanical interaction. Maximum sagging of bone under screw's head ranged between 0.10 and 0.13 mm*

For the same reason, all screws were tightened with a force of 80 N at the screw's head and bone contact surface. The femur model was fully constrained at its base. A set of loads of 3150 N distributed over the joint surface, 900 N at 15 degrees medially to the vertical axis and 1165 N at 30 degrees laterally to the vertical axis, were applied to the femoral head to simulate the loading conditions caused by the joint reaction and the contraction of the gluteus maximus and the gluteus medius muscles, respectively, during average daily activities (MOW and HAYS, 1997).

FE meshes of 250–300 or 800–1000 plate elements (2D, four nodes) were produced for the idealised models and the femoral head models, respectively. Finer meshing was produced at the screw–bone interface zones to improve the accuracy of the numerical solution (see Fig. 2*a*).

2.5 *Stress transfer parametric approach*

To quantify the screw–bone load transfer and its evolution with the adaptation of cancellous bone around the implant, two parameters, termed stress transfer parameters (STPs), were defined. These parameters α and β provide a convenient dimensionless evaluation of the load sharing between virtually any given fixation screw and the bone surrounding it (GEFEN, 2001; 2002)

$$\alpha = \frac{\sigma_{fb}}{\sigma_{ft}} \tag{4}$$

$$\beta = \frac{(1/N)\sum_{i=2}^{N}\sigma_{b_i}}{(1/N)\sum_{j=2}^{N}\sigma_{t_j}} = \frac{\sum_{i=2}^{N}\sigma_{b_i}}{\sum_{j=2}^{N}\sigma_{t_j}} \tag{5}$$

The above STP values were calculated as ratios of bone-averaged von Mises equivalent stress to screw-averaged stress in designated regions of interest, as demonstrated in Fig. 5. The stress transfer from the first (uppermost) thread of the screw, which bears an average stress of σ_{ft}, to the cancellous bone volume that is located directly above it and that can withstand an average stress of σ_{fb} is quantified by the α STP. The stress transfer from all the other threads of the screw (indexed as $j \geqslant 2$ to exclude the first thread), which bear respective stresses of σ_{t_j}, to the bone volumes (indexed i) that are found between these threads and that are withstanding respective stresses of σ_{t_i} is quantified by the β STP. As the bone is compressed between the first thread of the fixation screw and the head of the screw (Fig. 5), the first thread carries a disproportionately greater load that can cause stress concentrations to appear above it. For this reason, STP evaluations of the screw–bone stress transfer were carried out separately for the first thread (4) and for all the other threads (5).

The dimensionless STPs of (4) and (5) not only provide a practical tool evaluating biomechanical performances of specific familiar screw types with time, but also allow multi-comparisons and the subsequent rating of existing and theoretical designs. Ideally, if screws were made of a material with properties identical to those of bone, the screw and the bone would share similar loads, and a nearly homogeneous stress transfer would result. In such a case, stress shielding would be eliminated, bone resorption due to reduced loading would be unlikely, and the values of the above-defined STPs ((4) and (5)) would approach an optimum magnitude of unity. Indeed, both the idealised and femur model simulations used herein provided values of 0.96–0.99 for both α and β ratios ((4) and (5)) when modelling was carried out using different hypothetical screws with triangular, rectangular or trapezoidal profiles fabricated from a material with an elastic modulus identical to that of cancellous bone (around 1 GPa).

In contrast, for screws with lower biomechanical compatibility (e.g. those that are significantly stiffer than bone), lower STP values were obtained. By this means, the dimensionless STPs were utilised to rate the different commercial/theoretical screw designs (Section 2.3) and to identify the design parameters that are most critical for better long-term biomechanical performances.

To present the STP data as a function of the time course, we followed the experimental results of JEE (1983), who reported a bone turnover rate of 7.6% per year (total bone loss forms 100%

in 13 years). As the maximum change in apparent density with each time step is known and equals 0.04 g cm^{-3}, then, according to (1) and (3), a single computational iteration represents the elapse of 74 days (10.6 weeks).

3 Results

The remodelling algorithm described in Section 2.2 was activated for each screw design, using the idealised and femoral head models. The effects of the different design features on the screw–bone load sharing and predicted adaptation response of the bone tissue are detailed as follows.

3.1 *Screw–bone stress transfer*

For all the designs tested, namely titanium or reduced-stiffness titanium screws with triangular, rectangular or trapezoidal profiles and different lengths, diameters and numbers of threads (as detailed in Section 2.3), the greatest stress concentrations (10–25 MPa) appeared in the cancellous bone around the first (uppermost) thread of the screw. This stress concentration is a result of the screw's head being fastened to the cortical surface, causing the bone bounded between the head and the first thread to be firmly compressed (Fig. 5). For the trapezoidal and triangular profiles, some of these focal stresses were also distributed around the first thread's tip to the bone between it and the lower, second thread. In contrast, for the rectangular profile and, particularly, for the one with a wide thread diameter, stresses tended to be concentrated above the first thread, without extending to the lower threads.

Increasing the number of threads for a given screw design generally yielded more continuous stress transfer between the screw and bone, as evidenced by an increase in the STP values. Accordingly, the β STP values of the nine-thread models were higher by 21% on average, compared with those of the five-thread models. The stress distribution on the cortical bone surface (of the idealised models) also improved when the eight- and nine-thread screws were used, which provided a lower peak stress under the screw's head for each of the three different profile shapes tested (for instance, there was a 33% reduction in the maximum stress value for a nine-thread trapezoidal profile shape compared with a similar four-thread screw).

3.2 *Simulations of loosening process for commercial screw designs*

An important result of the present simulations is the characterisation of the time course of the loosening process. Loosening of a screw will begin to occur in places where bone density drops below the critical value (determined as being 0.01 g cm^{-3}). For all the commercial designs tested, cancellous bone resorption is predicted to initiate between the two most distal threads of the screw; this process then progresses upward, along the screw's shaft.

Figure 6 describes the evolution of the von Mises stress distribution in an idealised screw–bone model of a triangular-shaped screw profile. It can be seen that, as the density of bone around the tip of the screw decreases, the stress level in its vicinity drops, thereby providing less stimulus for bone maintenance around the upper threads. This leads to progressive resorption of the bone that is bounded between the uppermost adjacent threads. Following 70 weeks in simulation terms, the threads at the distal third of this screw had completely lost their structural support (i.e. the cancellous bone density around them equalled 0.01 g cm^{-3}). Under these screw–bone interface conditions, the screws were assumed to be loosened, the screw's micromotion was considered as now being possible (as in Fig. 1*b*), and the simulation was terminated. Based on these Figures, Table 1 details predicted loosening periods for common commercial screw designs when they are inserted into the femoral head.

3.3 *Performances of graded-stiffness and active-compression screws*

A representative evolution of the von Mises stress distribution in the cancellous bone around a graded-stiffness screw, as predicted by the femoral head model, is shown in Fig. 7. The evolution of the STP values against time is shown in Fig. 8 for the commercial screw types and in Fig. 9 for the innovative graded-stiffness and active-compression screw types.

As described in Section 2.5, greater values of the STPs are desired (and should be maintained for as long as possible), so as to afford an optimum sharing of loads between the fixative screw under evaluation and the surrounding cancellous bone. According to the STP criteria applied to the commercial screws, the best conditions post-implantation (PI), in terms of the average thread-to-bone stress transfer β, were provided by the wide-threaded triangular screw ($\beta = 0.652$ immediately PI). However, when 40 weeks were simulated to have elapsed, its stress transfer performances deteriorated and became similar to those of the screws with a trapezoidal profile.

The superior performances of the graded-stiffness and active-compression screw types, from the perspective of screw-to-bone stress transfer, were evidenced by the results of the STP analysis (Fig. 9), which demonstrated significantly smaller fluctuations (15% maximum) in their load sharing with bone owing to tissue adaptation (compared with changes of up to 70% that were observed for the commercial designs). The wide, rectangular active-compression screw presented the optimum load sharing with cancellous bone in its vicinity: the bone volume above the first thread carried stresses that were nearly the same (90–98%) as those of the first thread itself, and the bone volumes confined between the other threads of this screw were loaded in descending order by as much as 53–47% of the internal thread stress values, performances that were maintained until the simulation reached a steady state.

The latter findings indicate the potential for improving the biomechanical compatibility of bone screws using this design type, compared with commercially available screws in which the average thread–bone load sharing deteriorated from 65% at best to around 35–15% within 40 weeks or less.

4 Discussion

In the present study, dynamic simulations of bone adaptation were applied to predict cancellous bone resorption around orthopaedic fixative implants. The adaptation process, controlled by mechanosensors within the bone structure, was identified as an important cause of the implant's loosening and undesirable micromotion that had been documented in both animal experiments and clinical studies (SKINNER and POWLES, 1986; PANAGIOTOPOULOS *et al.*, 1994). Because the stress-shielding patterns causing the adaptation are dependent upon the material and geometrical characteristics of the fixative screw, the nature of the resultant bone resorption should also depend upon the physical design of the screw. It stands to reason that screw designs can be optimised, in terms of selecting appropriate geometric and material properties that would produce minimum bone loss.

Two FE model types, i.e. idealised axisymmetrical bone bulk and a femoral head structure into which different fixation screws were inserted, were selected for this study to predict bone stresses around the screw. In general, comparative STP evalua-

tions of different screw designs were found to be independent of the modelling approach, as the relative rating of the screw performances was maintained when either idealised or femoral head models were used. However, the absolute STP values obtained for the femoral head models were significantly larger than those obtained for the idealised models. For instance, using the idealised modelling approach, a 4 mm titanium screw with a trapezoid profile obtained a score of 0.24 and 0.50 immediately PI for the α and β STPs, respectively, whereas the femoral head model yielded scores of 0.52 and 0.74 for these α and β STPs, respectively. This indicates that the realistic load sharing between the screw and the surrounding bone is actually better than predicted using our idealised modelling approach.

The complex system of loads that acts on a screw within the proximal femur is not limited to axial forces along the screw's shaft, but also involves bending and shearing forces that simultaneously apply additional stress stimuli to promote the maintenance of bone around and between the screw's threads. In view of these factors, it was concluded that maintaining consistency in the modelling approach is a basic condition for comparing the STPs in different screw designs.

The trapezoidal and triangular profiles were shown to distribute the screw–bone contact stresses around the first thread toward the second thread and downward along the screw's axis, whereas, in the rectangular profile, stresses tended to be concentrated above the first thread without extending downward. The transfer of some of the local highly elevated stresses resulting from tightening of the screw to the lower threads in the trapezoidal and triangular screw geometries seems beneficial, not only for minimising the risk of damage to the bone trabeculae above the first thread, but also for providing some mechanical stimulus to the bone elements bounded between the lower threads, and thus increasing the potential for adequate osseointegration of the implant.

Table 1 Predicted time to screw loosening for various commercial screw designs (all with shaft length of 75 mm) inserted into proximal femur. For simulation purposes, screw is considered loosened when density of cancellous bone around distal third of its length decreases to 0.01 g cm^{-3}

Screw type	Simulation predictions of time to expected loosening, weeks
Triangular	75
Triangular, wide	85
Trapezoidal	95
Trapezoidal, wide	106
Rectangular	95
Rectangular, wide	149

Increasing the number of threads from five to eight or nine significantly reduced the peak stress under the screw's head (by 30–35%) for each of the three different profile shapes tested. Therefore longer screws, with eight or more threads, should be preferred where possible to minimise the risk of micro-cracking of the bone under the head while the screw is being tightened.

Utilising the criterion of elapsed time until loosening (Section 2.2), the wide trapezoidal and wide rectangular profile shapes emerge as being preferable among the commercial designs. However, the graded-stiffness and active-compression screw types demonstrate substantially improved performances, compared with the commercial designs. The more homogenous stress transfer provided by the graded-stiffness screw for main-

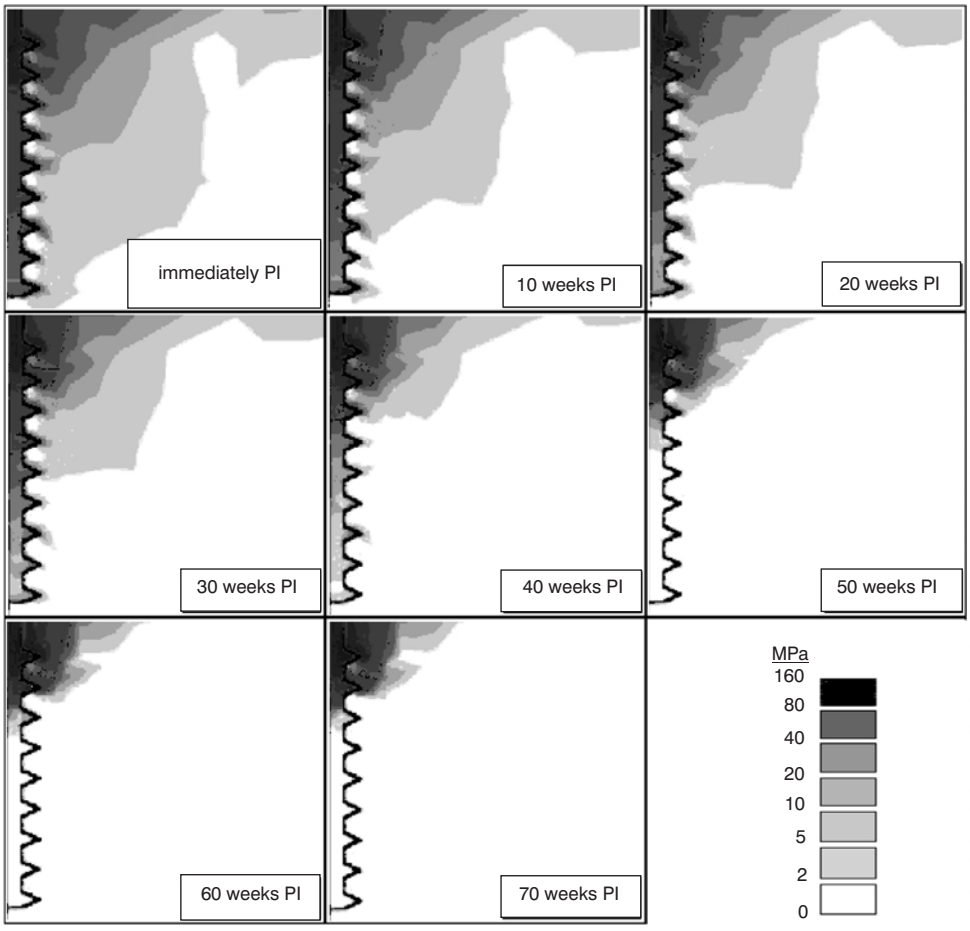

Fig. 6 *Evolution of von Mises stress distribution in cancellous bone around screw with triangular-shaped nine-thread profile, as predicted by idealised axisymmetrical screw–bone model. PI-post-implantation*

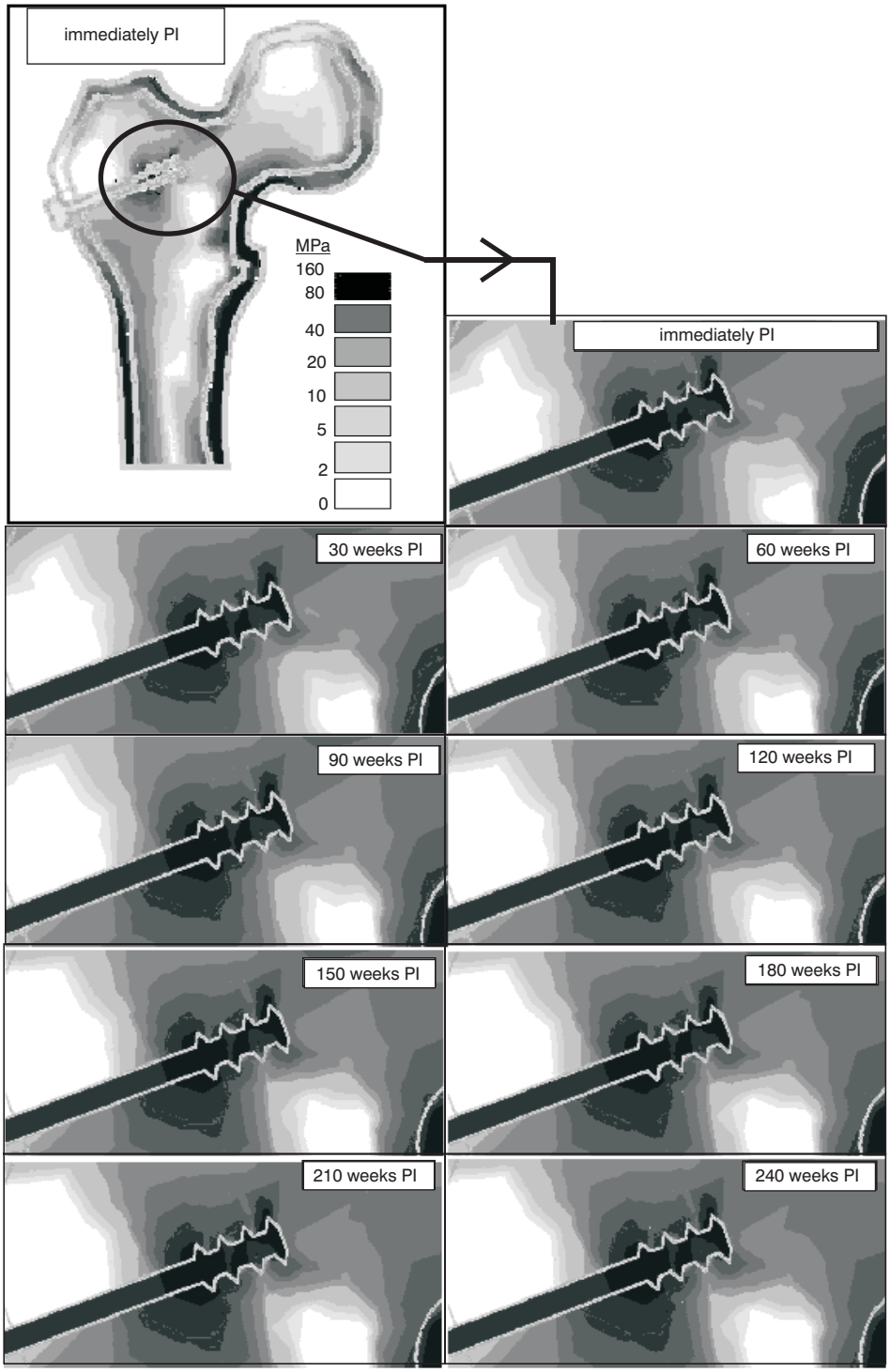

Fig. 7 *Evolution of von Mises stress distribution in cancellous bone around graded-stiffness screw with short shaft and triangular-shaped four-thread profile, as predicted by femoral head screw–bone model. Stress distribution within entire femoral head immediately post-implantation (PI) is seen in top left corner and is followed by PI time-series of magnifications of stress field development in cancellous bone in vicinity of threads*

tenance of the surrounding bone yielded a completely steady state of adequate cancellous bone density around the screw's threads (0.6–1.2 g cm^{-3}) after 240 weeks (in simulation terms). This result indicates that no significant bone resorption would be likely to occur between the graded-stiffness screw's threads throughout the complete lifetime of the implant.

Figure 7 illustrates this finding by showing the stress field evolution around a triangular-shaped thread profile for a graded-stiffness screw inserted into the proximal femur. Although some changes (of up to 5 MPa) in the stress field as a result of bone adaptation can be observed above the screw's shaft in the proximity of the greater trochanter, as well as around the lower femoral neck, the stress distribution between and around the screw's threads is very steady.

Several alternatives can be considered for manufacturing a suitable biocompatible polymeric layer for the graded-stiffness screw. A first approach can be to select ultra-high molecular-weight polyethylene (UHMWPE), which is very wear resistant and thus can reduce scraping of debris during insertion of the screw (PRENDERGAST, 2000). A second, promising approach could be to use a bio-absorbable polymer (poly-L-lactite acid (PLLA)). Theoretically, an absorbable material for the outer layer of the graded-stiffness screw appears to be beneficial, as, while the outer layer gradually decomposes and is replaced by

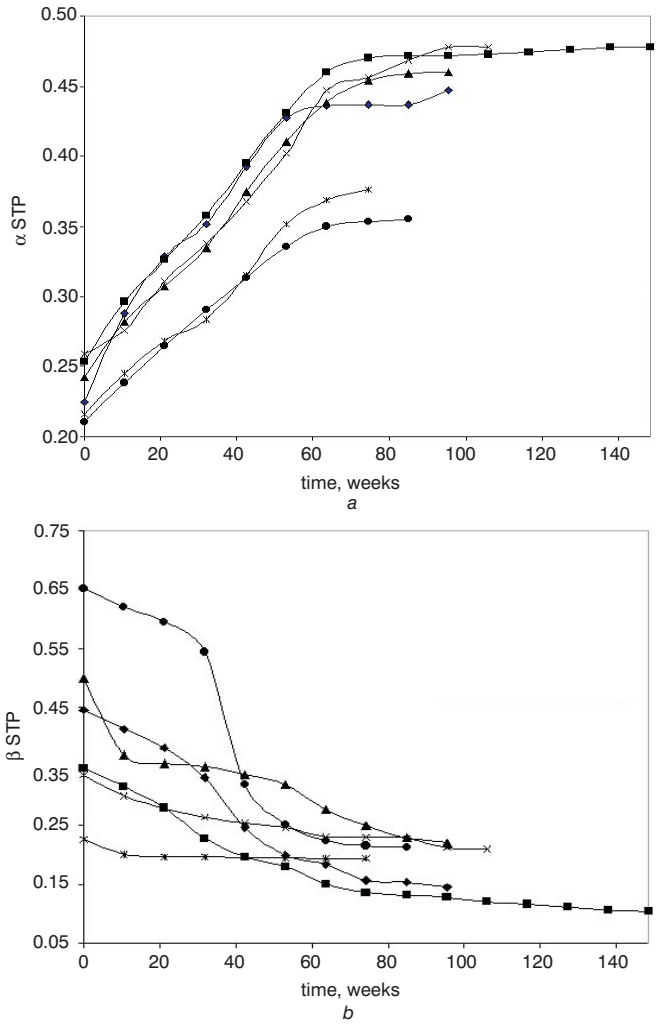

Fig. 8 *Evolution of stress transfer parameters (STPs) for bone adaptation behaviour around different commercial nine-thread screw designs, as predicted by idealised axisymmetrical model type: (a) stress transfer between first thread and cancellous bone volume above it, in terms of α STP (4); (b) averaged stress transfer between all screw threads (excluding first one) and cancellous bone volume bounded between threads, in terms of β STP (5).* (—◆—) *Rectangular;* (—■—) *rectangular wide;* (—▲—) *trapezoid;* (—×—) *trapezoid wide;* (—✳—) *triangular;* (—●—) *triangular wide*

bone, stresses are also gradually transferred, so that minimum stress shielding will occur. The use of PLLA for pins in foot and ankle surgery was lately reported to be well tolerated by patients (THORDARSON *et al.*, 2001). However, a recent study by COLLINGE *et al.* (2000) suggested that PLLA has a poor resistance to torsion loading and therefore could be damaged by the torques that are applied during insertion of the screw and that are partially transferred to the coating from the titanium core. Experimental *in vitro* evaluations (e.g. insertion and pull-out tests) and *in vivo* animal studies of the level of osseo-integration should be the subject of future studies for testing the clinical applicability of the graded-stiffness design.

The computational results of this study can be compared with histomorphological evaluations in the literature. SCHULLER-GÖTZBURG *et al.* (1999) presented histological images from two patients who underwent median splitting of the mandible to treat carcinoma of the mouth. The specimens with the screws were retrieved at re-operation (3 months post-implantation) because of local recurrence of the tumors. All the screws in their study had a triangular profile. It is evident from the images of SCHULLER-GÖTZBURG *et al.* (1999) that the majority of bone resorption took place around the tip of the screws, and that no bone contacts existed in most of the threads of its distal third. Resorption directly under the screw's head and along the upper part of the shaft was minimal.

These findings strongly support the behaviour of the present computational simulations, which predict that the loosening begins at the tip of the screw, progressing upward along its shaft (see Section 3.2). The simulations also predict that, for a triangular profile, this process should last about 70 weeks, whereas the images of SCHULLER-GÖTZBURG *et al.* (1999) demonstrate that the major deterioration in the screw's stability appears after (only) 12 weeks. One possible explanation for the time differences concerns the computational algorithm, which could not fully mimic the real coupling between bone resorption, micromotion of the screw, inflammation and further resorption. As the simulated response of the tissue in the models includes the effects of stress stimulations, but not the effect of the screw's micromotion (which further damages the adjacent delicate trabecular structures), the simulated time course for loosening appears to be longer than the observed one. Nevertheless, a major advantage of the model simulations is their ability to isolate and demonstrate the effects of stress shielding and the resulting reduced stress stimulus on the resorption process.

The present screw–bone computational models are based upon several assumptions that should be taken into account when interpreting the results. For example, the adaptation algorithm that was employed (Fig. 3) relates local bone stiffness to the respective bone density, according to (1) (CARTER and HAYES, 1977). Some experimental variability had been found in

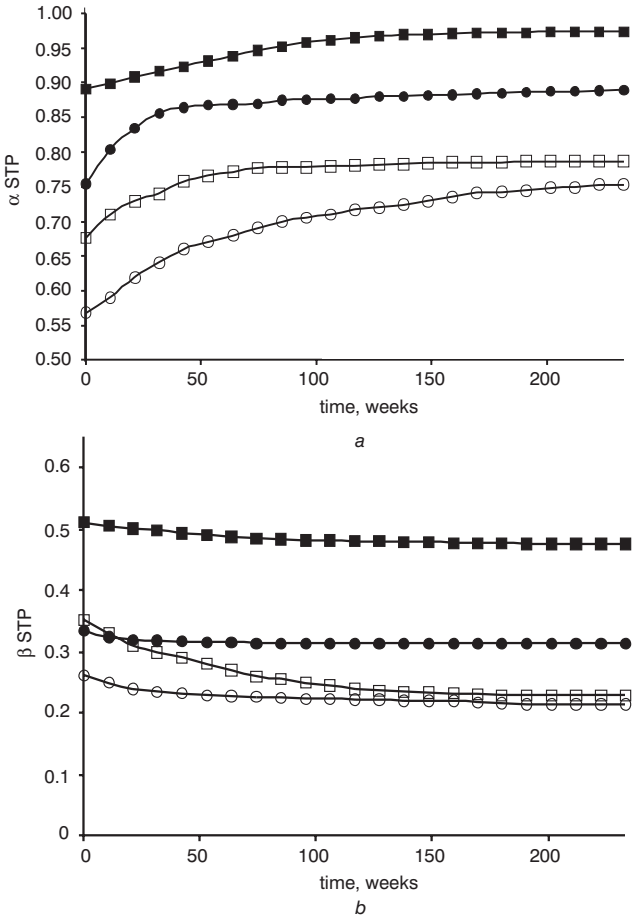

Fig. 9 *Evolution of stress transfer parameters (STPs) for bone adaptation behaviour around newly proposed graded-stiffness and active-compression nine-thread screws, as predicted by idealised axisymmetrical model type: (a) stress transfer between first thread and cancellous bone volume above it, in terms of α STP (4); (b) averaged stress transfer between all screw threads (excluding first one) and cancellous bone volume bounded between threads, in terms of β STP (5). (–■–) Active-compression wide rectangular; (–●–) active-compression triangular; (–□–) graded-stiffness wide rectangular; (–○–) graded stiffness triangular*

the stiffness–density relationship (HUISKES *et al.*, 1992; VAN REITBERGEN *et al.*, 1993). These differences are mainly related to the porous characteristic of the cancellous bone, which indicates a degree of dependency upon the sites from which specimens are taken. A sensitivity analysis of the models to variations of up to 15% in the proportion coefficient of the stiffness–density relationship of (1) (taken as 2875 MPa cm^3g^{-1}, from CARTER and HAYES (1977)) did not introduce significant changes in the results, in terms of the evolution of stress distribution within the bone, the pertinent STP evolution and the predicted progress of implant loosening.

The present models did not take into account the true trabecular micro-architecture of the cancellous bone, but rather assumed it to consist of a homogenous isotropic material. Accordingly, determining the local effects of the screw's engineering design on the microstructural stress distribution and the adaptation pattern of individual trabeculae awaits further studies. Additional limitations stem from the utilisation of 2D models, given that real-life screw–bone mechanical interaction is 3D. Nevertheless, the suggested methodology and, in particular, the STP evaluation approach are applicable for future 3D computational analyses.

In summary, a method of evaluating and rating engineering designs and expected biomechanical performances of orthopaedic fixative screws has been presented. The results indicated that wide (6 mm thread diameter) rectangular and trapezoidal screw profiles have superior biomechanical compatibility with bone compared with the other commercially available profile types that were tested. The promising computational STP results obtained for the graded-stiffness and active-compression screw designs will have to be validated with data from animal experiments. Finally, the present work demonstrated that bone-remodelling computer simulations can be used as a highly effective tool for the evaluation of several design parameters of the screws, such as geometry, material characteristics and others.

Acknowledgments—This study was supported by the Ela Kodesz Institute for Medical Engineering & Physical Sciences and by the Internal Fund of Tel Aviv University, Israel. Y. Gotlieb and M. Shabtai are thanked for their help in developing the computational models. Esther Eshkol is thanked for her editorial assistance.

References

ADAMS, C. I., ROBINSON, C. M., COURT-BROWN, C. M., and MCQUEEN, M. M. (2001): 'Prospective randomized controlled trial of an intramedullary nail versus dynamic screw and plate for intertrochanteric fractures of the femur', *J. Orthop. Trauma*, **15**, pp. 394–400

ALBREKTSSON, T., (1985): 'Bone tissue response', in 'Tissue-integrated prostheses' (Quintessence Publishing, Chicago, IL, 1985), pp. 129–144

ANG, K. C., DAS DE S., GOH, J. C., LOW, S. L., and BOSE, K. (1997): 'Periprosthetic bone remodelling after cementless total hip replacement. A prospective comparison of two different implant designs', *J. Bone Joint Surg. (Br)*, **79**, pp. 675–679

BEAUPRÉ, G. S., ORR, T. E., and CARTER, D. R. (1990): 'An approach for time-dependent bone modeling and remodeling – application: a preliminary remodeling simulation', *J. Orthop. Res.*, **8**, pp. 662–670

CARTER, D. R., and HAYES, W. C. (1977): 'The compressive behavior of bone as a two-phase porous structure', *J. Bone Joint Surg. (Am)*, **59**, pp. 954–962

CARTER, D. R., ORR, T. E., and FYHRIE, D. P. (1989): 'Relationships between loading history and femoral cancellous bone architecture', *J. Biomech.*, **22**, p. 231

COWIN, S. C., and HEGEDUS, D. H. (1976): 'Bone remodeling I: theory of adaptive elasticity', *J. Elasticity*, **6**, p. 313

COLLINGE, C. A., STERN, S., CORDES, S., and LAUTENSCHLAGER, E. P. (2000): 'Mechanical properties of small fragment screws', *Clin. Orthop.*, **373**, pp. 277–284

EVANS, M., SPENCER, M., WANG, Q., WHITE, S. H., and CUNNINGHAM, J. L. (1990): 'Design and testing of external fixator bone screws', *J. Biomed. Eng.*, **12**, pp. 457–462

GEFEN, A. (2001): 'Dynamic simulations of cancellous bone resorption around orthopaedic fixative implants'. Proc. of 23rd Annual International Conference of IEEE Engineering in Medicine & Biology Society, October 25–28, Istanbul, Turkey

GEFEN, A. (2002): 'Optimizing the biomechanical compatibility of orthopaedic screws for bone fracture fixation', *Med. Eng. Phys.*, **24**, pp. 337–347

GUE, X. E. (2001): 'Mechanical properties of cortical bone and cancellous bone tissue', in COWIN, S. C. (Ed.): 'Bone mechanics handbook' (CRC Press, Boca Raton, Florida, 2001), pp. (10)1–23

HUISKES, R., WEINANS, H., GROOTENBOER, H. J., DALSTRA, M., FUDALA, B., and SLOOFF, T. J. (1987): 'Adaptive bone-remodeling theory applied to prosthetic-design analysis', *J. Biomech.*, **20**, p. 1135

HUISKES, R., WEINANS, H., VAN REITBERGEN, B., SUMMER, D. R., TURNER, D. M., and GALANTE, J. O. (1991): 'Validation of strain-adaptive bone remodeling analysis to predict bone morphology around noncemented THA'. Trans. 37th Annual ORS, Anaheim, California, March 4–7, **1**, p. 105

HUISKES, R., WEINANS, H., and VAN REITBERGEN, B. (1992): 'The relationship between stress shielding and bone resorption around total hip stems and the effects of flexible materials', *Clin. Orthop.*, **274**, pp. 124–134

HYLDAHL, C., PEARSON, S., TEPIC, S., and PERREN, S. M. (1991): 'Induction and prevention of pin loosening in external fixation: an in vivo study on sheep tibiae', *J. Orthop. Trauma*, **5**, pp. 485–492

JEE, W. S. S. (1983): 'The skeletal tissues' in WEISS, L. (Ed.): 'Histology: cell & tissue biology, 5th edn' (Elsevier, Amsterdam, 1983)

LEVENSTON, M. E., BEAUPRÉ, G. S., SCHURMAN, D. J., and CARTER, D. R. (1993): 'Computer simulations of stress-related bone remodeling around noncemented acetabular components', *Arthroplasty*, **8**, pp. 595–605

LOWERY, G. L., and MCDONOUGH, R. F. (1998): 'The significance of hardware failure in anterior cervical plate fixation. Patients with 2- to 7-year follow-up', *Spine*, **23**, pp. 181–187

MOW, V. C. and HAYS, W. C. (1997): Basic orthopaedic biomechanics (Lippincott-Raven, Philadelphia, PA, 1997)

OMURA, T., TAKAHASHI, M., KOIDE, Y., OHISHI, T., YAMANASHI, A., KUSHIDA, K., and INOUE, T. (2000): 'Evaluation of isolated fractures of the greater trochanter with magnetic resonance imaging', *Arch. Orthop. Trauma Surg.*, **120**, pp. 195–197

PANAGIOTOPOULOS, E., FORTIS, A. P., MILLIS, Z., LAMBIRIS, E., KOSTOPOULOS, V., and VELLIOS, L. (1994): 'Pattern of screw loosening in fractures fixed with conventional and functional plates', *Injury*, **25**, pp. 515–517

PERREN, S. M., CORDEY, J., BAUMGART, RAHN, B. A., and SCHATZKER, J. (1992): 'Technical and biomechanical aspects of screws used for bone surgery', *Int. J. Orthop. Trauma*, **2**, pp. 31–48

PILLIAR, R. M., CAMERON, H. U., BINNINGTON, A. G., SZIVEK, J., and MACNAB, I. (1979): 'Bone ingrowth and stress shielding with a porous surface coated fracture fixation plate', *J. Biomed. Mater. Res.*, **13**, pp. 799–810

PRENDERGAST, P. J. (2000): 'Bone prostheses and implants' in COWIN, S. C. (Ed.): 'Bone biomechanics handbook' (CRC Press, Boca Raton, Florida, 2000), pp. (35)1–29

SCHULLER-GÖTZBURG, P., KRENKEL, CH., REITER, T. J., and PLENK, H. JR. (1999): '2D-finite element analyses and histomorphology of lag screws with and without a biconcave washer', *J. Biomech.*, **32**, 511–520

SKINNER, P. W., and POWLES, D. (1986): 'Compression screw fixation for displaced subcapital fracture of the femur. Success or failure?', *J. Bone Joint Surg. (Br)*, **68**, pp. 78–82

TERRIER, A., RAKOTOMANANA, R. L., RAMANIRAKA, A. N., and LEYVRAZ, P. F. (1997): 'Adaptation models of anisotropic bone', *Comput. Methods Biomech. Biomed. Eng.*, **1**, pp. 47–59

Thordarson D. B., SAMUELSON, M., SHEPHERD, L. E., MERKLE, P. F., and LEE, J. (2001): 'Bioabsorbable versus stainless steel screw fixation of the syndesmosis in pronation-lateral rotation ankle fractures: a prospective randomized trial', *Foot Ankle Int.*, **22**, pp. 335–338

TOMITA, N., and KUTSUNA, T. (1987): 'Experimental studies on the use of a cushioned plate for internal fixation', *Int. Orthop.*, **11**, pp. 135–139

TOMITA, N., KUTSUNA, T., TAMAI, S., UDEA, Y., IKEUCHI, K., and IKADA, Y. (1991): 'Mechanical effects of a cushioned plate on bone fixation', *BioMed. Mater. Eng.*, **1**, pp. 243–250

VAN REITBERGEN, B., HUISKES, R., WEINANS, H., SUMMER, D. R., TURNER, T. M., and GALANTE, J. O. (1993): 'The mechanism of bone remodeling and resorption around press-fitted THA stems', *J. Biomech.*, **26**, pp. 369–382

WIMMER, C. and GLUCH, H. (1998): 'Aseptic loosening after CD instrumentation in the treatment of scoliosis: a report about eight cases', *J. Spinal Disord.*, **11**, pp. 440–443

Author's biography

Dr AMIT GEFEN is a Lecturer in the Department of Biomedical Engineering at the Faculty of Engineering of Tel Aviv University, Israel. He received his BSc in Mechanical Engineering, in 1994, his MSc and PhD in Biomedical Engineering, in 1997 and 2001, respectively, from Tel Aviv University. His experience is in foot and gait biomechanics, as well as in bone biomechanics and in the application of computational modelling methods to the design and biomechanical optimisation of implants.